

General Disclaimer

One or more of the Following Statements may affect this Document

- This document has been reproduced from the best copy furnished by the organizational source. It is being released in the interest of making available as much information as possible.
- This document may contain data, which exceeds the sheet parameters. It was furnished in this condition by the organizational source and is the best copy available.
- This document may contain tone-on-tone or color graphs, charts and/or pictures, which have been reproduced in black and white.
- This document is paginated as submitted by the original source.
- Portions of this document are not fully legible due to the historical nature of some of the material. However, it is the best reproduction available from the original submission.

NASA Technical Memorandum 86870

(NASA-TM-86870) PLASMA DEPOSITED
DIAMONDLIKE CARBON ON GaAs AND InP (NASA)
15 p HC A02/MF A01 CSCL 20L

N85-10844

G3/76
Unclas
24199

Plasma Deposited "Diamondlike" Carbon on GaAs and InP

J. D. Warner, J. J. Pouch, S. A. Alterovitz,
and D. C. Liu
*Lewis Research Center
Cleveland, Ohio*

and

W. A. Lanford
*SUNY-Albany
Albany, New York*



Prepared for the
Thirty-first National Symposium of the American Vacuum Society
Reno, Nevada, December 3-7, 1984

NASA

I. INTRODUCTION

There has been considerable interest in the properties of carbon films¹⁻⁷ prepared by ion-beam sputtering¹⁻⁶ and rf plasma decomposition of hydrocarbon gases.³⁻⁵ Information on film hardness and bonding arrangements (relative to diamond) can be found in the literature.²⁻⁶ Recently, some optical and electrical characteristics of carbon films grown on Si, which may be useful for semiconductor applications fabrication, have been reported.^{1,4,8,9}

We have utilized a rf plasma formed from methane gas to deposit the carbon films. The physical and chemical properties of these films have been determined using AES, XPS, ellipsometry, nuclear reaction techniques, IR and UV-vis-NIR spectrometries. Our results provide information on the growth parameters needed to achieve carbon films with a particular bandgap and hydrogen content. In addition, we demonstrate the importance of the growth temperature on the deposition rate and composition.

II. EXPERIMENT

a. Growth and Sample Preparation

Carbon films were prepared by subjecting the substrates to a rf plasma discharge generated at 30 kHz. We used a Technics PD-II deposition system. All samples were first cleaned in acetone and ethanol baths, and rinsed in deionized water. The samples were then placed in the rf chamber; the background pressure was typically 20 mtorr. Methane gas (99.97 percent pure) was used to flush the chamber several times prior to each run. The power and flow rate settings were varied from 30 to 240 W and from 30 to 90 sccm, respectively; substrate temperatures ranged from ambient (~23° C) to 250° C. We noted that a minimum pressure was required to maintain a stable plasma and it scaled directly with rf power.

We report the measured quantities in flow rates with units of standard cubic centimeters (sccm) rather than pressure since it was the flow rate which was controlled during deposition. It was found that the pressure varies linearly with flow rate (f), in the region 30 to 90 sccm. To convert flow rate from sccm to pressure in mtorr we used the formula

$$P = 3.5f + 70 \quad (1)$$

where P is the pressure in mtorr. Carbon films were grown on GaAs, InP, Si wafers, quartz, and Multiple Internal Reflection (MIR) plates of Ge and Si. All samples were stored either under vacuum or in a dry box.

b. AES/ESCA

The composition analyses experiments were performed using a PHI AES/ESCA system, interfaced with a MACS (Multiple-Technique Analytical Computer System). The sample chamber was evacuated to about 10^{-10} torr prior to the Auger electron profiling and X-ray photoemission measurements. The sputter profiling was done with 2 or 3 KeV Ar ions at 25 mA. The XPS measurements were carried out using a 10 KeV Al K_{α} x-ray source.

c. IR

Determination of the relative amount of hydrogen in the film was performed using a ratio recording infrared spectrometer with a data station for data acquisition and analysis of the peak area. The area under the absorption peaks at 2921, 1444, and 1374 cm^{-1} were used. These measurements were taken in the spectrometer using Ge and Si MIR plates with a 30° bevel on the two ends. In order to reduce the edge effects and assure the uniformity of the film across the MIR plates, an aluminum plate of approximately the same thickness as the MIR plates was placed around the plates during deposition. These peaks gave the main vibrational and bending modes of the C-H_x ($x = 1$ to 3) bondings.

d. Optical Absorption

Optical absorption measurements were done on carbon films deposited on fused quartz plates to determine the bandgap. The films were measured in a UV-vis-NIR spectrometer with the sample beam perpendicular to the film. The wavelength was scanned from 185 to 836 nm with a bandwidth of 1 nm and a scan rate of 5 nm/sec while the background was automatically subtracted.

e. Ellipsometry

Optical properties such as the refractive index and the thickness of the films were determined using a semi-automatic Gaertner L119X research ellipsometer in a rotating analyzer mode. Data acquisition and analysis were done using a computer. At each wavelength, up to nine angles of incidence were used, as needed. The light sources were a He-Ne laser and a 100 W Hg arc source. The photomultiplier readings were averaged over at least 50 rotations, with a measurement every 5° of the analyzer, at each wavelength and angle of incidence.

The thickness and the complex refractive index at 632.8 nm were measured systematically on a large number of samples. On each sample, data was obtained at angles of incidence in the range of 60° to 78°. From these measurements ψ and Δ were calculated by Fourier analysis. In some samples several wavelengths were used. Then the refractive index and the thickness were calculated from a multiple angle and wavelength (MAW) program developed at the University of Nebraska.¹⁰ The optical data for the substrate were taken from literature.¹¹ A three-phase model was used, i.e., ambient, film, and substrate. This model was found very adequate for our films.

f. Nuclear Reaction

Determination of the absolute amount of hydrogen was performed at the Suny-Albany nuclear accelerator. This method makes use of the 4.43 MeV γ -rays emitted from the $H^1(N^{15}, \alpha\gamma)C^{12}$ reaction. This reaction has an appreciable cross section for N^{15} nucleon only ions at 6.385 MeV. The method of calculating the hydrogen concentration from this reaction is given in Ref. 12.

III. RESULTS

AES and XPS measurements indicated that the films contained only carbon; no other element was observed to the detection limits (0.1 at. %) of the instrument. Figure 1 shows a typical AES profile of carbon films on InP and GaAs. Oxygen was present only on the surface of the films for the GaAs samples whereas for the InP there was a few percent of oxygen at the carbon-InP interface. This suggests that the methane plasma removes all of the oxygen from the GaAs surfaces and most of it from InP surfaces.

Our analysis of the percent diamondlikeness of our films comes from the measurement of the asymmetry in the carbon 1s XPS lineshape due to delocalized π -bonds.¹³ To quantify this measurement, we compare the relative asymmetry in the C 1s spectrum of our samples to that of Highly Oriented Pyrolytic Graphite (HOPG). We define the percent diamondlikeness (DL) to be

$$DL = (1 - \alpha_1/\alpha_2) \times 100 \quad (2)$$

where α_1 is the area of the tail relative to the total area of the symmetric peak for the sample, and α_2 is the area of the tail relative to the total area of the symmetric peak for HOPG. The measurement value for α_2 is 0.25. In Figure 2, we show a comparison of the XPS peaks of HOPG, a

plasma deposited carbon film, and a Gaussian curve fitted to the low energy side of the peak for the carbon film.

The DL calculated for the various carbon films ranged from 40 to 97 percent. There is a general trend of decreasing DL values with increasing power/flow rate values.

The XPS evaluation of the bonding of the carbon to GaAs and InP were performed with films approximately 200 Å thick. The results for a typical film on InP is shown in Fig. 3. The interface was extending approximately from 5 to 20 min ESCA profiling time. Data were taken at 8 and 14 min. All XPS peaks are broadened and shifted in binding energy for material at the interface, as compared to the bulk. This includes the C 1s, the In 3d and P 2p peaks, indicating some bonding between the carbon and the InP. Similar behavior was found at the carbon-GaAs interface.

Using a rf power of 100 W and a flow rate of 50 sccm with Si and Ge substrates it was found that the carbon growth rate and hydrogen concentration decreases with increase in substrate temperature as measured by the N^{15} nuclear reaction. Figure 4 shows for carbon on Si that the deposition rate falls off exponentially with temperature whereas the hydrogen concentration decreases linearly with temperature. Deposition rates were determined from measurements of film thickness by a standard profilometry technique. For InP and GaAs, it was found that the carbon growth rate decreases with increasing temperature and above 200° C nucleation does not occur.

The carbon films on Si and Ge MIR plates show a decrease in the intensity of the infrared absorptive peaks, with increasing temperature. The IR data show peaks around 2921 cm^{-1} for $C-H_x$ ($x = 1$ to 3) stretching modes, peaks at 1445 cm^{-1} and 1370 cm^{-1} for the $C-H_2$ and $C-H_3$ bending modes, and a broad peak at 1610 cm^{-1} which is probably associated with amorphous carbon

modes. The absorption intensities of the C-H_x peaks can be used to determine the hydrogen concentration once the thickness and optical absorption cross section of the C-H_x peaks are known. The optical absorption cross section for these films will be reported elsewhere.¹⁴ Figure 5 illustrates the sensitivity of the IR optical absorption intensity of the C-H_x peaks due to changes in Ge substrate temperature.

The ellipsometric measurements of index of refraction (n) and extinction coefficient (k), for films produced at rf powers of 50 and 240 W and methane flow rates of 30 to 90 sccm, together with deposition rates from the ellipsometric measured thickness, are given in Table I. The growth rate increased for both rf power and methane flow rate. The index of refraction decreased slightly with flow rate and increased with power. The extinction coefficient at 6328 Å was nonzero only at the lowest flow rate whereas at shorter wavelengths for the 50 W and 90 sccm samples, k was measurable but is still quite small.

The change in the index of refraction in samples prepared at different power levels could be due to changes in concentration of voids from sample to sample. To check this we used the effective medium approximation¹⁵ to calculate the concentration of the voids and the required AES profiling time for several samples. Assuming that the 240 W, 50 sccm sample has no voids we calculate the percent voids (PV) in other samples. For example, we found PV = 45 for the 50 W, 90 sccm sample. This value leads to calculated AES profiling time of 108 min as compared with the experimental value 105 min. We thus obtained a ratio of 3.5 for the profiling time, as compared to a factor of 2.0 for the thickness ratio.

The optical bandgap results for various power flow rate ratios are given in Figure 6. They range from 2.07 to 2.38 eV and decrease with increase in

power/flow rate for a given power. This tendency is the same as for the percentage diamondlike behavior shown in Figure 3.

IV. SUMMARY

We have demonstrated that reasonably high purity and quality carbon film can be produced on GaAs and InP over a wide range of rf power and methane flow rate. These films show no impurities other than hydrogen. We found a tendency for the carbon films to be more diamond at lower ratios of rf power to methane flow rates. We were able to control the bandgap and growth rate of the films through reproducible settings of power and flow rate. We have shown the exponential decrease of the growth rate and a decrease of the hydrogen concentration with increase in substrate temperature during deposition on Si and Ge substrates. Also, we observe a critical temperature (200° C) above which no nucleation of carbon occurs on GaAs and InP.

More work is needed on carbon films prepared by rf glow discharge to fully determine the variation of the bandgap and growth rate during deposition with the parameters rf power, methane flow rate, and temperature. In addition, the relationship between the bandgap, index of refraction, and the amount of either voids or hydrogen in the films should be investigated.

ACKNOWLEDGMENTS

We would like to thank John A. Woollam and collaborators at University of Nebraska-Lincoln for fruitful discussions and technical help.

REFERENCES

1. A. A. Khan, J. A. Woollam, Y. Chung, and B. Banks, *IEEE Electron Device Letters*, **4**, 146 (1983).
2. C. Weissmantel, K. Bewilogua, D. Dietrick, H. J. Erler, H. J. Hinneberg, S. Klose, W. Nowick and G. Reisse, *Thin Solid Films*, **72**, 19-31, (1980).
3. C. W. Weissmantel, G. Reisse, H. J. Erler, F. Henny, K. Bewilogua, U. Ebersback, and C. Shurer, *Thin Solid Films*, **63**, 315-325 (1979).
4. D. Mathine, R. O. Dillon, A. A. Khan, G. Bu-Abbud, J. A. Woollam, D. C. Liu, B. Banks, and S. Domitz, *J. Vac. Sci. Technol.*, **A2**, 365-366 (1984).
5. T. J. Moravec and T. W. Orent, *J. Vac. Sci. Technol.* **18**, 226-228 (1981).
6. C. Weismantel, K. Bewilogua, K. Brewer, D. Dietrick, U. Ebersback, H. J. Erler, B. Rau, and G. Reisse, *Thin Solid Films*, **96**, 31-44 (1982).
7. S. Aisenberg and R. Chabot, *J. Appl. Phys.*, **42**, 2953-2958 (1971).
8. R. O. Dillon, J. A. Woollam, and V. Katkanant, *Phys. Rev.* **B29**, 3482-3489 (1984).
9. Y. Ichinose and F. Shimokawa, in Extended Abstracts and Program, 16th Biennial Conference on Carbon, (American Carbon Society, University Park, Penn, 1983).
10. G. H. Bu-Abbud, S. A. Alterovitz, N. M. Bashara, and J. A. Woollam, *J. Vac. Sci. Technol.* **A1**, 619-620 (1983).
11. D. E. Aspnes, and A. A. Studna, *Phys. Rev.* **B27**, 985-1009 (1983).
12. T. T. P. Cheung, *J. Appl. Phys.*, **53**, 6857-6862 (1982).
13. W. A. Lanford, and M. J. Rand, *J. Appl. Phys.* **49**, 2473-2477 (1978).
14. J. D. Warner, W. A. Lanford, J. J. Pouch, and S. A. Alterovitz, to be published.
15. D. E. Aspnes, *Thin Solid Films*, **89**, 249-262 (1982).

ORIGINAL PAGE IS
OF POOR QUALITY

TABLE I. - ELLIPSOMETRY DATA OF CARBON FILMS AT 6328 Å

Sample		Deposition rate, Å/min	Index of refraction, n	Extinction coefficient, k
Power, W	Flow rate, cm			
50	30	79.5	1.58±0.02	-0.01
50	50	83.3	1.71±.02	0
50	70	96.7	1.67±.01	0
50	90	100.0	1.59±.02	0
240	50	197	2.15±.04	-.015
240	70	263	2.08±.09	0
240	90	308	1.81±.01	0

ORIGINAL QUALITY
OF POOR QUALITY

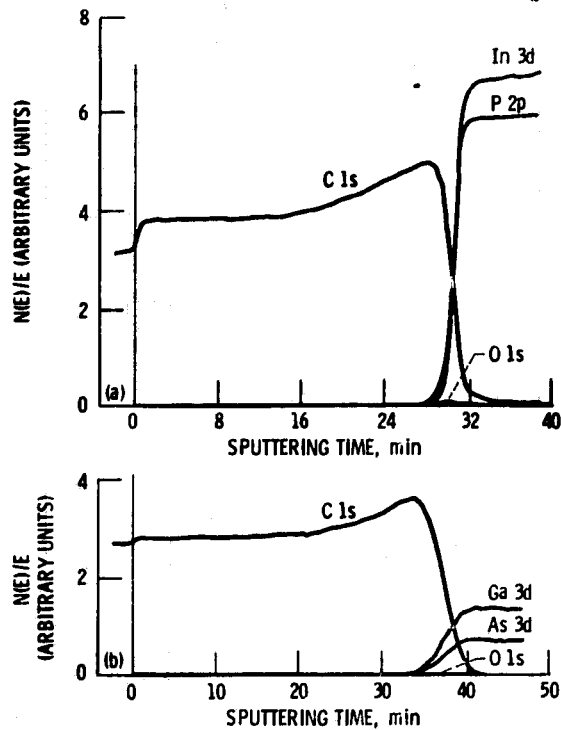


Figure 1. - Auger electron spectroscopy (AES) profiles of carbon films on InP (curve A) and GaAs (curve B), using 25 mA, 3 keV Ar ions.

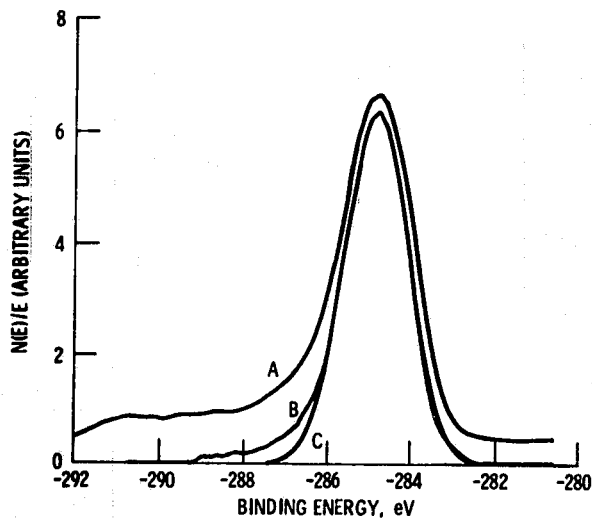
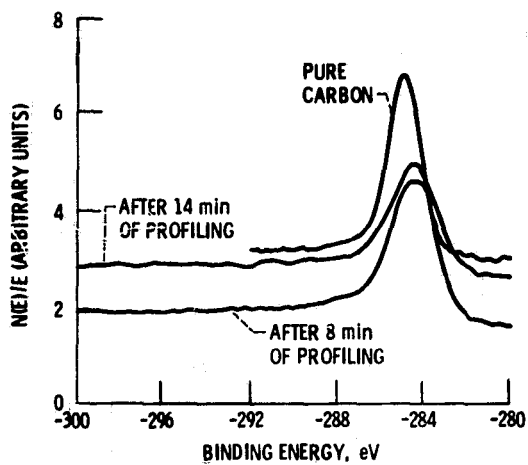
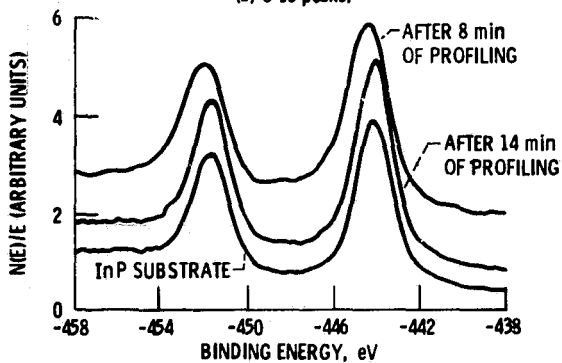


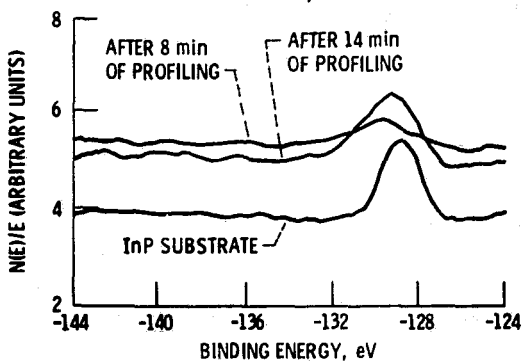
Figure 2. - X-ray photoemission spectroscopy (XPS) of the intensity of photoemission electrons versus binding energy. (A) - highly oriented pyrolytic graphite (B) - carbon film on InP, (C) - fitted gaussian curve to the lower energy side of curve (B).



(a) C 1s peaks.



(b) In 3d peaks.



(c) P 2p peaks.

Figure 3. - XPS intensity versus binding energy at different depth of profiling time for carbon film of thickness of 200 Å on InP.

ORIGINAL ...
OF POOR QUALITY

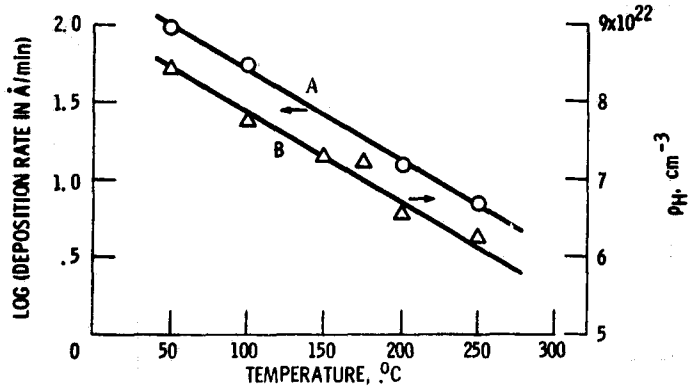


Figure 4. - Logarithmic plot of deposition rate versus temperature (A) and hydrogen concentration ρ_H (atoms per cm^3) versus temperature (B) for carbon on a Si substrate with growth parameters: 100 W, 50 sccm, and 30 min.

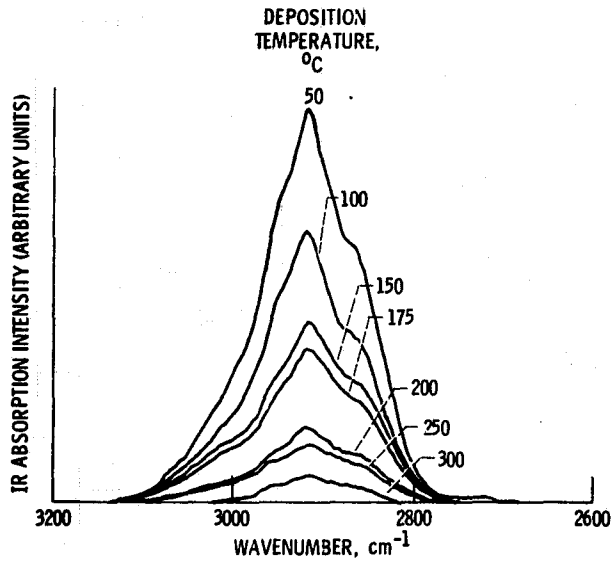


Figure 5. - IR absorption intensity versus wavenumber for carbon on Ge MIR (multiply internal reflection) plates for 7 deposition temperatures at 100 W, 50 sccm, and 30 min.

ORIGINAL PAGE IS
OF POOR QUALITY

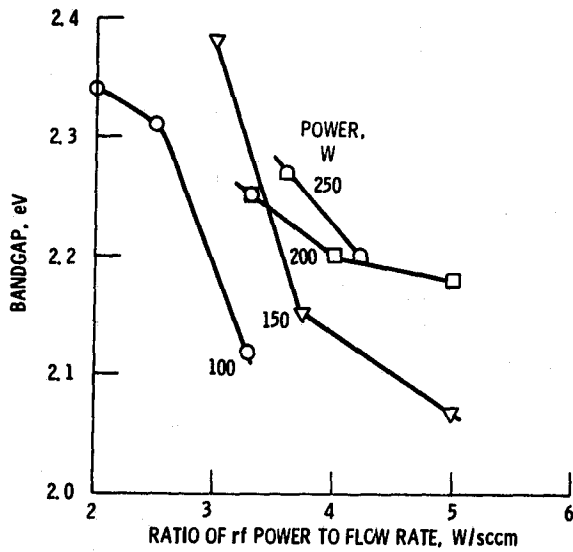


Figure 6. - Optical bandgap versus the ratio of rf power (W) and flow rate (sccm) for different power levels.